Journal of Manufacturing Engineering, June, 2014, Vol. 9, Issue. 2, pp 071-076

COMPARATIVE EVALUATION OF TEMPERATURE DISTRIBUTION IN GTAW AND FSW JOINTS OF AA 5059 ALUMINIUM ALLOY

[*]Babu N[1], Karunakaran N[2] and Balasubramanian V[3]

[1]Assistant professor, Department of Mechanical Engineering, Annamalai University, Annamalai Nagar-608002.Tamil Nadu, India
[2] Associate professor, Department of Mechanical Engineering, Annamalai University, Annamalai Nagar-608002.Tamil Nadu, India
[3] Professor, Department of Manufacturing Engineering, Annamalai University, Annamalai Nagar-608002.Tamil Nadu, India

ABSTRACT

AA 5059 alloy is best suited for military applications because of high strength to weight ratio and high toughness. Also this high magnesium content aluminium alloy is used to make ship hull structure because of good corrosion resistance and good strength. Hence this study aimed to experimentally explore the thermal history of a work piece involving gas tungsten arc welding and friction stir welding. K-type thermocouples are used to record the temperature history at six different locations on work piece. The results of these analyses indicate that low temperature values were recorded in FSW process compared to GTAW process. The results of the simulation are in good agreement with that of experimental results.

Key words*: Friction stir welding, Gas tungsten arc welding, Temperature distribution, Finite element analysis.*

1. Introduction

Aluminium alloy AA 5059 is newly developed armour grade aluminium alloy which is mainly recommended in the ship hull and super structure due to its beneficial properties like high corrosion resistance, high strength to weight ratio, formability, etc.[1]. The aluminium is welded successfully using GTAW and FSW process. GTAW is a high heat input welding process which was applied locally along the weld line. Due to the uneven heat distribution, their induced residual stress in the system. Similarly, due to difference in the plastic strain in weld nugget and elastic strain in the neighboring region, their induced residual stress in FSW. The uneven distributions of heat make the material to expand and contract. This results a geometrical instability in the weld joint called distortion [2-8].

Some researchers have proposed analytical models and experimental methods to explore the temperature distribution within the work piece during the welding process. Infrared cameras are usually used to measure temperature distribution during FSW. However, only the temperature distribution on the surface of the work piece can be obtained using this method. Thermocouples are the mostly commonly used sensor for measuring temperature histories inside the work piece. However, the temperature along the joint line cannot be obtained during FSW, because the thermocouples could be destroyed by the tool when it traverses through the joint line. Although the heat input of FSW is lower than that of fusion welding, it is still a process accompanied with uneven heating and cooling, so the presence of residual stress and distortion is inevitable[9-14]. In GTAW process, the high heat generation may melt the thermocouple. The heat input rate is one of the most important variables in fusion welding and can strongly affect phase transformations during welding. Because, it governs heating rate, cooling rate and weld pool size. The metallurgical feature that is directly affected by heat input rate is the grain size in the heat affected zone (HAZ) and in the weld metal. Therefore understanding the thermal histories and temperature distributions in the work piece is an important issue, not only to verify whether a process will be employed, but also because it influences the residual stress, the grain sizes, and accordingly, the strength of the welds. Thus the heat generation, subsequent heat distribution and heat loss to the ambient should be known for the better understanding of residual stress and distortion formation in a welded joint. It is observed that very few research works are carried out in predicting the temperature distribution on AA 5059 alloy welded joints. Hence, the present research work focuses on the temperature distribution of friction stir welded and gas tungsten arc welded AA 5059 aluminium alloy joints in order to evaluate the joint performance and the weld zone characteristics.

**Corresponding Author - E- mail: babu.manu11@gmail.com*

2 Experimental Work

The base material used in this work was AA 5059 aluminum alloy. The chemical composition of the base material is evaluated by using vacuum spectrometer (ARL model 3460). Sparks were ignited at various locations, and their spectrum was analyzed and the estimated alloying elements are presented in Table 1. The base material mechanical properties are shown in Table 2. In this investigation, two welding process namely conventional GTAW and solid state FSW are used for the investigation. The base material was prepared into dimensions of 150 × 75 × 4 mm for both the weld. The process parameters used for GTAW and FSW to make defect free joints are shown in Table 3. After numerous trials, the joint which was free of volumetric defect and other defect like crack, inclusions, etc was considered as the optimized condition for both GTAW and FSW joints. K type thermocouples made of chromel and alumel with a sensitivity of 41 μV/°C was used for temperature prediction. In order to embed the thermocouples, holes are drilled to a depth of 2 mm at three different location 7 mm, 12 mm, and 17 mm away from the weld centre line and along the mid length at both side of the plate. The temperature evolution during welding was measured and interpreted using data acquisition system and recorded in the computer by the use of Lab View software.

2.1 Finite element analysis

A three-dimensional nonlinear thermo-mechanical analysis is carried out using welding simulation finite Element code COMSOL. In order to reduce the computational time and improve the accuracy of result, finer mesh was carried out near the weld region and gradient coarser mesh was carried out away from the weld region. Dissimilar meshed model of elements were used for finite element analysis The meshed model composed of quadrilateral elements, triangular elements, prism elements, edge elements and vertex elements.

Table 1: Chemical Composition of base Material AA 5059

Si	Fe	Cu	Mn	Mg	Zn	Ti	Al
0.041	0.1	0.003	0.933	5.21	0.001	0.489	Remaining

Table 2: Mechanical Properties of base Material AA 5059

Yield strength, MPa	Ultimate tensile strength, MPa	Elongation in 50 mm gauge length	Micro hardness $HV_{0.5}$
350	395	9	123

Table 3: Welding Condition and Optimized Process Parameters

Parameters	GTAW	FSW
Tungsten electrode diameter (mm)	3	-
Voltage (Volts)	20	-
Current(amps)	145	-
Welding speed (mm/s)	2.04	1.85
Shielding gas	Argon	-
Gas flow rate (l/min)	20	-
Tool rotational speed (rpm)	-	980
Axial force (kN)	-	3.0
Tool shoulder		12 mm
Tool pin		4 mm
Tool material		HSS

2.1.1 Mechanical boundary condition

The specified mechanical boundary conditions are those just sufficient to prevent rigid body motion of the model. Zero displacement conditions were used for constraining the butt joint which resembled the complete fixed fixturing.

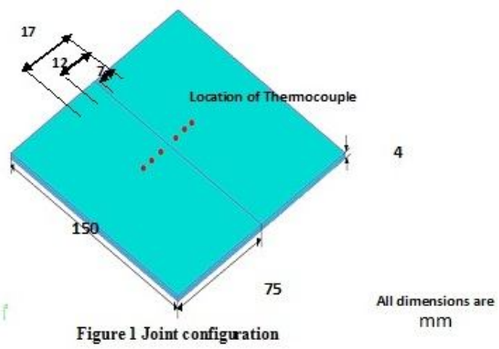

Figure 1 Joint configuration

Fig 2.a. GTAW

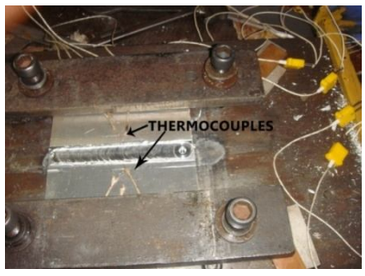

Fig 2.b. FSW

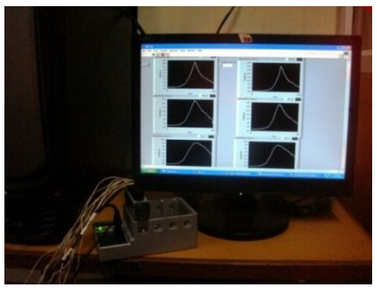

Fig 2.c. Data acquisition system

Fig. 2 Temperature measuring system

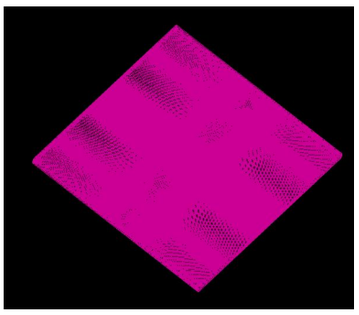

Fig 3.a Meshed Model - GTAW

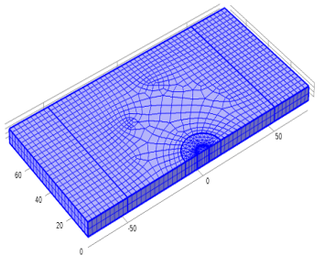

Fig 3.b Meshed Model - FSW

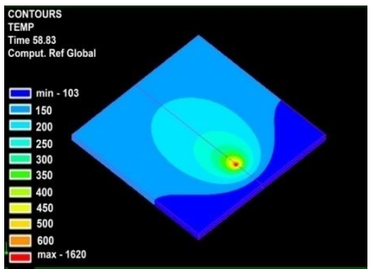

Fig 3.c Simulated Model – GTAW

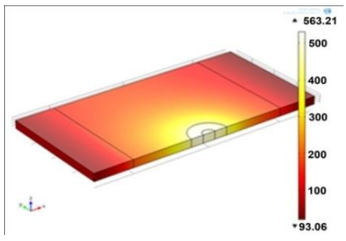

Fig 3.d Simulated Model - FSW

Fig 3. FEA resuts

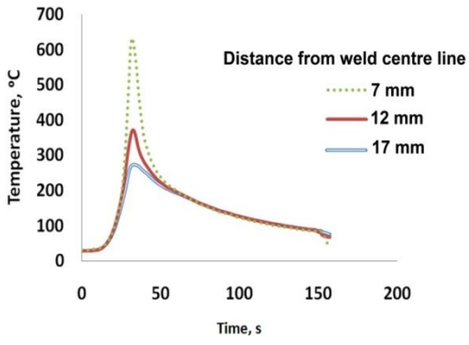

Fig. 4 Temperature profile of GTAW (Experimental)

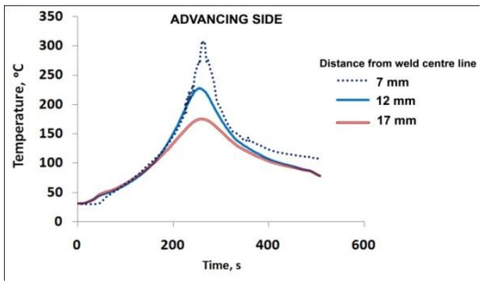

Fig 5.aTemperature profile of FSW (Experimental) (Advancing side)

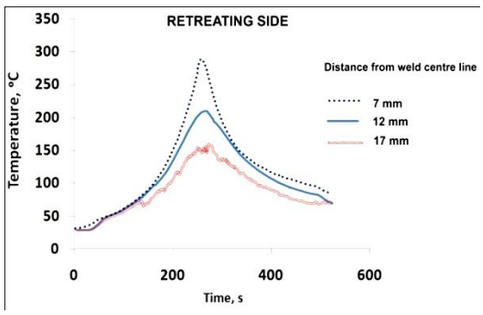

Fig 5.b Temperature profile of FSW (Experimental) (Retreating side)

2.1. 2 Thermal boundary condition

For both GTAW and FSW process, the samples are clamped at the backing plate. Thus the heat generated during welding was lost due to heat conduction. The governing differential equation for three dimensional heat conduction equations for a solid in Cartesian coordinate system is given by

$$\frac{\delta^2 T}{\delta x^2}+\frac{\delta^2 T}{\delta y^2}+\frac{\delta^2 T}{\delta z^2}+\frac{q_g}{x}=\frac{1}{\propto}\left(\frac{\delta T}{\delta t}\right) \quad (1)$$

Where, $\alpha = \frac{k}{\rho C_p}$ thermal diffusivity of the material, q_g is the heat generation per unit volume in W/m^3, ρ is density of the material in kg/m^3; C_p is specific heat in J/kgK and k are thermal conductivity W/mK.

Heat loss from all the other surface are assumed as heat loss due to natural convection and surface-to-ambient radiation at the free surface was considered and the corresponding heat flux expression for these surfaces are

$$q = h(T_0 - T) + \varepsilon\sigma(T_{amb}^4 - T^4) \quad (2)$$

Where, Heat transfer coefficients for natural convection, T_0 is an associated reference temperature, ε is the surface emissivity, σ is the Stefan-Boltzmann constant, and T_{amb} is the ambient air temperature.

2. 2 Heat source modelling of GTAW

The moving heat source is represented as moving the heat generation of the nodes in each computational time step. John Goldak et al.[16] proposed heat source model called double ellipsoid heat source model which use heat flux as the thermal load with ramping function. It is seen from, it was concluded that the double ellipsoid heat source model is the only model which imitate the exact size and shape of weld bead made by GTAW process.

$$q_f(x,y,z,t) = \frac{6\sqrt{3}f_f Q}{abc_f\pi\sqrt{\pi}} exp\left\{-3\left(\frac{x^2}{a^2}+\frac{y^2}{b^2}+\frac{(z+vt)^2}{c_{f^2}}\right)\right\} \quad (3)$$

$$q_r(x,y,z,t) = \frac{6\sqrt{3}f_r Q}{abc_r\pi\sqrt{\pi}} exp\left\{-3\left(\frac{x^2}{a^2}+\frac{y^2}{b^2}+\frac{(z+vt)^2}{c_{r^2}}\right)\right\} \quad (4)$$

Q_f is the energy input to the front quadrant of the ellipsoid in Watts per cubical millimetre, Q_r is the energy input to the rear quadrant of the ellipsoid in watts per cubical millimetre, a, b, c_f and c_r are the Gaussian parameters.

2.3 Heat source modelling of FSW

The heat generated is concentrated locally and d5str5b4ted into subsequent regions of the plates by heat conduction according to (Equation 1) as well as convection and radiation through the boundary. Three-dimensional heat transfer model assumes the tool shoulder and pin have a constant heat flux. Heat generation in shoulder-work piece interface involves the interactive effect major element such as vertical pressure, area subjected to friction, angular velocity, etc. It can be mathematically expressed as

$$q_s = (\mu \times F/A_s) \times (R \times \omega) \quad (5)$$

Where, F represents the normal force, A_s is the shoulder's surface area, μ is the friction coefficient, R is the distance from the center axis of the tool and ω is the angular velocity of the tool (rad/s).

The model simulates the heat generated in the interface between the tool's pin and the work piece as a surface heat source pin-work piece interface.

Where, μ is the friction coefficient, r_p denotes the pin radius, ω refers to the pin's angular velocity (rad/s), and Ybar(T) is the average shear

$$q_p = \mu / sqrt\left(3 \times (1 + \mu^2)\right) \times \left(r_q \times \omega\right) \times Ybar(T) \quad (6)$$

3. Results and Discussion

3.1 Temperature history

Figure 3 shows the finite element results of GTAW and FSW process. The thermo-mechanical non linear simulation of welding process is modelled and analyzed. Figure 3c shows the contour plot of FE-GTAW process. In GTAW, higher temperature of 1620°C was observed at the weld bead due to the melting of materials. The thermal gradient of higher temperature to lower temperature and their distribution from weld centre to away materials were clearly observed by the difference in color contours. Due to high thermal conductivity, the heat generated at the weld centre due to welding is readily transferred to the neighboring region. Because of this, the differences in temperature with respect to distance were changed at every instance as the weld ramp proceeds.[16]. Figure 3d shows the contour plot of FE-FSW process. In FSW, higher temperature of 563°C was observed at the stir zone due to the stirring action of the rotating pin and forging action of the shoulder.. Since the heat generated at the weld centre is relatively lower than the GTAW process, smoother thermal gradient were observed. In FSW, the difference in temperature from the weld centre to any direction is lower than GTAW process.. The double ellipsoid heat source model clearly replicate the actual shape and size of the weld bead and HAZ region of GTAW process. Similarly, the trapezoidal form of stir zone formed during FSW . .Nandan et al.[16] reported that Peak temperatures in the work-piece are attained close to the edge of the tool shoulder in FSW.

Fig.4.shows temperature distribution of GTAW process based on the experiment results at an optimized process parameter. The maximum temperature of experimental result that detected for 7 mm from the center of weld was approximately 620 ºC which is slightly lower than melting point of base material. At 12 mm and 17 mm away from the center of the weld experimental temperature values recorded around 390°C and 270°C respectively. However, it can be noted that the temperature decreased with increasing distance from the weld center.

Fig.5.shows temperature values of FSW process which was measured by thermocouples. Some important observations can be made from this plot First, maximum temperature was recorded at the locations close to the stirred zone. Also maximum temperature was recorded at advancing side (320°C) compared to retreating side (290°C). The measured temperature between these two sides is less since this base material has high thermal conductivity. Because the material on the retreating side never enters into the rotational zone near, but the material on the advancing side forms to fluidized bed near the pin and rotates around it. After several revolutions the material on the advancing side is very highly deformed and sloughs off behind the pin. Second, maximum temperature rise within the weld zone is below the melting point of aluminium. Compared to GTAW process, temperature measured in FSW process is low.

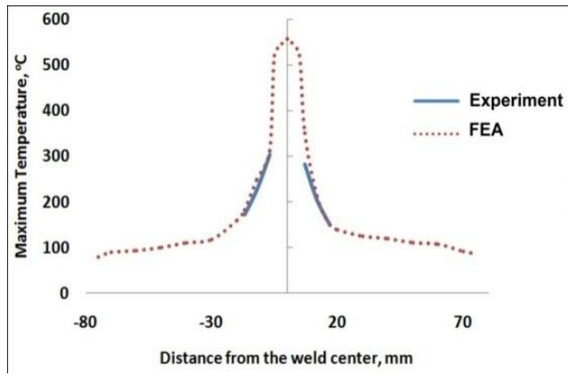

Fig.6.a. Validation of FEA results with experimental (GTAW)

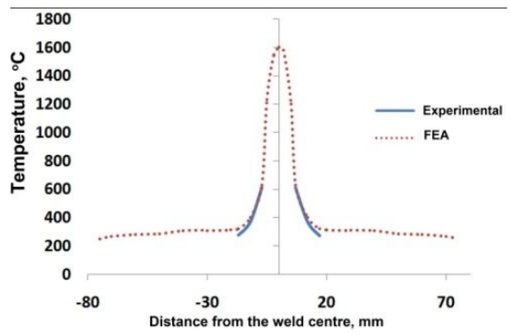

Fig.6.b. Validation of FEA results with experimental (FSW)

Figure.6 compares the predicted and measured temperature history for weld which was produced with optimized process parameters. It can be observed that the experimental and numerical temperature distributions match fairly well.

4. Conclusions

In this paper, finite element models have been developed to analyze the temperature distributions in conventional GTAW and unconventional FSW processes. Thermal histories have been predicted and compared with experimental results.

i. In GTAW, higher temperature of 1620°C was observed at the weld bead, whereas in FSW process 563°Cwas observed at the stir zone due to the stirring action of the rotating pin and forging action of the shoulder. The heat generated at the weld centre is relatively lower than the GTAW process, smoother thermal gradient were observed.

ii. The temperatures on the advancing side were slightly higher than those on the retreating side in FSW process because the material that experiences the highest strain and strain rate is on the advancing side of the weld.

References

1. *Anderson T (2003), "New developments within the Aluminium Shipbuilding Industry", Svetsaren, Vol.58, 3-5.*
2. *Bugáacki H (1999), "Wpáyw technologii spawania na odpornoĞü korozyjną stopów Al-Zn-Mg", International Conference On ":Environmental Degradation of Engineering Materials", Politechnika GdaĔska, 260-267.*
3. *Czechowski M (2007), "Effect of anodic polarization on stress corrosion cracking of some aluminium alloys", Advances in Materials Science, Vol. 7, 1 (11), 13-20.*
4. *Czechowski M, Pietras A and Zadroda L (2003), "The Properties of Aluminium Alloys 5xxx Series Welded by New Technology Friction Stir Welding", InŀynieriaMateriaáowa, Nr 6 (137), 264-266, Advances in Materials Science, Vol. 7, 1(11).*
5. *Davis J R (1999), "Corrosion of Aluminium and Aluminium Alloys", ASM International, Materials Park, OH.*
6. *John goldak Malcolm Bibby, Moore J, House R, and Patel B (2009), "Computer Modeling of heat flow in welds", Metallurgical Transactions B 1984, Vol 15B.*
7. *Czechowski M, Chrzanowski J, ZieliĔski, et.al (2001), "NaprĆŀeniowe konferencja Naukowa - InŀynieriaMateriaáowa Politechnika GdaĔska", Sobieszewo.*
8. *Jata K V, Semiatin S L, (2001), "Continuous dynamic recrystallization during friction stir welding of high strength aluminum alloys", Scripta Mater Vol. 43, 743e9.*
9. *Bowden F P, Hughes T P, Hughes (1999), Proc,R.Soc.London,Ser.A "Dimensional¯ow and thermal modeling of the friction stir welding process. In. Proceedings of the 2nd International Symposium on Friction Stir Welding, Sweden.*
10. *Bendzsak G B, North T H and Smith C (2000), "InProceedings of the 2nd International Symposium on Friction Stir Welding, Sweden.*
11. *Smith C B, Bendzsak G B, North T H, Hinrichs J F, Noruk J S and Heideman R J (2000), Heat and material, In. Proceedings of ninth International Conference on Computer Techology in Welding.*
12. *Krishnan K N (2006), "Onion formation in friction stir welds".*
13. *Wert J A et.al. (2003), "Microstructures of friction stir weld joint between aluminium base metal matrix composite and amonolithic aluminium alloy".*
14. *Attallah M M , Davis C L , Strangwood M (2000), Proceedings of the 6th international symposium on friction stir welding Saint sauveur,TWI.*
15. *Lomolino et al. (2008), "Effects of friction stir welding on microstructure of 6061-T6 aluminium alloy".*
16. *Nandan M (2003), et. al. WáasnoĞci záączy doczoáowych blach ze stopów Al- Mg spajanych róŀnymi metodami, Materiaáy i Technologie, Politechnika GdaĔska, Nr 1(1), 16-19, GdaĔsk.*
17. *Goswami R, Spanos G, Pao P S, Holtz R L (2010), "Precipitation behavior of the beta phase in Al-5083", Mat. Sci. Eng. A-Struct., Vol. 527, 1089e95.*
18. *Chen C M, Kovacevic R, Jandgric D, Wavele E (2008), "Transform analysis of acoustic emission in monitoring friction stir welding of 6061 aluminum"; Vol. 43, 1383e90.*

